Science of the Total Environment 809 (2022) 151132

Contents lists available at ScienceDirect

Science of the Total Environment

journal homepage: www.elsevier.com/locate/scitotenv

Pollution characteristics, exposure assessment and potential cardiotoxicities of $PM_{2.5}$-bound benzotriazole and its derivatives in typical Chinese cities

Chun Yang [a], Shiyao He [a], Shimin Lu [a], Xiaoliang Liao [a], Yuanyuan Song [b], Zhi-Feng Chen [a], Guoxia Zhang [c], Ruijin Li [d], Chuan Dong [d], Zenghua Qi [a,*], Zongwei Cai [a,b,**]

[a] Guangdong-Hong Kong-Macao Joint Laboratory for Contaminants Exposure and Health, School of Environmental Science and Engineering, Institute of Environmental Health and Pollution Control, Guangdong University of Technology, Guangzhou 510006, China
[b] State Key Laboratory of Environmental and Biological Analysis, Department of Chemistry, Hong Kong Baptist University, Hong Kong, China
[c] Department of Environmental Health, Guangdong Provincial Key Laboratory of Tropical Disease Research, School of Public Health, Southern Medical University, Guangzhou 510515, China
[d] Institute of Environmental Science, Shanxi University, Taiyuan, China

HIGHLIGHTS

- Optimized methods of purification and GC–MS/MS were used to characterize $PM_{2.5}$-BTRs.
- The concentration of $PM_{2.5}$-BTRs in Taiyuan was the highest in three Chinese cities.
- Computational and experimental screening indicated 4TTR was the most harmful to NRCM.
- 4TTR activated the ROS-mediated mitochondrial apoptosis signaling pathway in NRCM.
- Metabolomics revealed that 4TTR disturbed mitochondrial energy metabolism in NRCM.

GRAPHICAL ABSTRACT

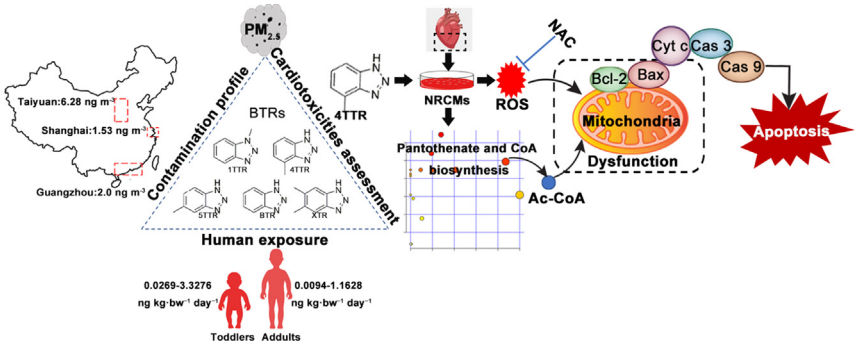

ARTICLE INFO

Article history:
Received 24 August 2021
Received in revised form 14 October 2021
Accepted 17 October 2021
Available online 22 October 2021

Editor: Jianmin Chen

Keywords:
$PM_{2.5}$
Benzotriazole
Pollution characteristic
Exposure risk
Cardiotoxicity

ABSTRACT

Benzotriazole and its derivatives (BTRs), classified as high-volume production chemicals, have been widely detected in various environmental media, including the atmosphere, water, soil and dust, as well as organisms. However, studies on the pollution characteristics and health impact of $PM_{2.5}$ related BTRs are so far limited. This study is the first to demonstrate the regional scale distribution of $PM_{2.5}$-bound BTRs and their potential cardiotoxicities. Optimized methods of extraction, purification and GC-EI-MS/MS were applied to characterize and analyze $PM_{2.5}$-bound BTRs from three cities in China during the winter of 2018. The concentration of $\sum$BTRs in Taiyuan (6.28 ng·m^{-3}) was more than three times that in Shanghai (1.53 ng·m^{-3}) and Guangzhou (1.99 ng·m^{-3}). Benzotriazole (BTR) and 5-methyl-1H-benzotriazole (5TTR) contributed more than 80% of $\sum$BTRs concentration as the major pollutants among three cities. The correlation analysis indicated that there was a positive correlation between temperature and concentration of BTR and a negative correlation between temperature and concentration of 5TTR. In addition, the risk of BTRs exposure to toddlers should be paid more attention in Taiyuan by the human exposure assessment. Furthermore, toxicity screening by experimental methods indicated that 4-methyl-1H-benzotriazole (4TTR) was the most harmful to cardiomyocytes. The western blot assay showed a ROS-mediated mitochondrial apoptosis signaling pathway was activated after exposure

* Correspondence to: Z. Qi, Rm 510, Engineering Facility Building No.3, School of Environmental Science and Engineering, Guangdong University of Technology, Guangzhou, China.
** Correspondence to: Z. Cai, Department of Chemistry, Hong Kong Baptist University, Hong Kong, China.
E-mail addresses: zenghuaqi@gdut.edu.cn (Z. Qi), zwcai@hkbu.edu.hk (Z. Cai).

https://doi.org/10.1016/j.scitotenv.2021.151132

to 4TTR in neonatal rat cardiomyocytes (NRCMs). On the other hand, metabolomics revealed that exposure of 4TTR to NRCMs disturbed mitochondrial energy metabolism by disturbing pantothenate and coenzyme A synthesis pathway. Our study not only clarifies the contamination profiles of $PM_{2.5}$-bound BTRs in typical Chinese cities but also reveals their cardiotoxicities associated with mitochondrial dysfunction.

1. Introduction

$PM_{2.5}$, particles with an aerodynamic diameter ≤ 2.5 μm, is a heterogeneous mixture with varying size and chemical composition depending on source, weather conditions, space and time. Due to the extremely small size and excellent adsorption capacity, $PM_{2.5}$ may be a dangerous carrier of affiliated chemicals owing to its rapid distribution throughout the body, including the brain, heart and other extrapulmonary organs (Qi et al., 2020). Organic matter of $PM_{2.5}$ has received increasing attention because of its environmental persistence, bioaccumulation and significant health risk. Although organic components are a major part of $PM_{2.5}$, only approximately 5–10% of them have been identified and quantified (Amrani et al., 2019; Turpin and Lim, 2001; Wu et al., 2018).

Benzotriazole and its derivatives (BTRs) are heterocyclic compounds with a basic structure of two fused rings and three nitrogen atoms. BTRs have excellent corrosion resistance, antifungal and UV absorption capacities, which makes them advantageous for many applications ranging from aircraft deicing/anti-icing fluids, washing powders and textiles to drugs and plastic products (Herrero et al., 2014; Janna et al., 2011; Liu et al., 2017; McNeill and Cancilla, 2009; Pena et al., 2012). Therefore, BTRs are widely used in our daily production and lives and are classified as high-volume production chemicals. Hundreds of tons of BTRs are produced and used annually in the USA and Australia, and global production and usage of BTRs will likely continue to grow in the future as economies further develop (Hart et al., 2004; Jia et al., 2019; Loi et al., 2013). However, the increased production of BTRs has also led to widespread accumulation in various environmental media, including the atmosphere, water, soil and dust, as well as organisms (Jia et al., 2019; Li et al., 2020; Loi et al., 2013; Loos et al., 2009; Shi et al., 2019; Weiss et al., 2006; Zhang et al., 2011). Worryingly, BTRs have been detected in human samples from around the world, including urine, amniotic fluid and adipose tissue (Asimakopoulos et al., 2013b; Asimakopoulos et al., 2013c; Garcia-Gomez et al., 2015; Wang et al., 2015). Recent studies have reported that 4-methyl-1H-benzotriazole (4TTR) and 5-methyl-1H-benzotriazole (5TTR) are the most prevalent BTRs in human samples (Li et al., 2018; Wang et al., 2015). Nevertheless, the specific ways in which BTRs enter the human body and their contribution remain unknown. In a recent review, Shi et al. suggested that more attention should be paid to BTRs exposure routes (Shi et al., 2019).

Exposure to BTRs might occur via multiple exposure routes, such as ingestion, dermal absorption and inhalation. Its main exposure sources to humans are contaminated food and water, textiles, and indoor and outdoor dust (Liu et al., 2017; Trabalon et al., 2017; Wan et al., 2016). BTRs usually suspend in the air via vapor and particulate phases. Xue et al. investigated the distribution differences of BTRs between vapor and particulate phases and found that air particulates have a strong adsorption capacity, especially for 5,6-dimethyl-1H-benzotriazole (XTR) (Xue et al., 2016). Additionally, the estimated daily intake (EDI) of BTRs for humans might depend on the size of particles. It has been hypothesized that $PM_{2.5}$-bound BTRs may be more harmful to human health by virtue of their adsorption and transport advantages, especially in Asia, where $PM_{2.5}$ is heavily polluted. However, previous studies aimed at monitoring $PM_{2.5}$-bound BTRs and their derivatives have mainly focused on limited areas, and few data are available regarding the regional and/or global scale distribution of $PM_{2.5}$-bound BTRs.

Owing to their frequent detection in environmental media and the human body, the toxicity of BTRs has attracted considerable interest in the past few years. A growing number of studies have reported the potential risks of BTRs to various organisms, e.g., microorganisms, plants, invertebrates and vertebrates, including hepatotoxicity, neurotoxicity, metabolic toxicity, reproductive and developmental toxicity, and carcinogenicity (Fent et al., 2014; Liang et al., 2017; Wang et al., 2017; Zhou et al., 2020). A recent study by Chen et al. demonstrated mitochondrial DNA copy number alternation in newborn babies' cord blood after pregnant women had been exposed to BTRs (Chen et al., 2020). Although, the heart possesses the highest content of mitochondria of any tissue to meet the enormous energy requirements and is a direct target organ for $PM_{2.5}$-bound organic components (Qi et al., 2020), the adverse effects of $PM_{2.5}$ related BTRs on cardiomyocytes and underlying mechanisms remain poorly investigated.

To address this knowledge gap, this study aimed to (a) identify contamination profiles of BTRs in urban $PM_{2.5}$ by establishing a set of analysis methods, (b) screen for potential exposure risks of $PM_{2.5}$ related BTRs, and (c) investigate the cardiotoxicities and underlying mechanisms by multiple approaches, including apoptosis analysis, untargeted metabolomics and mitochondrial function analysis.

2. Materials and methods

2.1. Chemicals and reagents

In this study, the target standards of five BTRs were investigated: 1H-benzotriazole (BTR), 1-methyl-1H-benzotriazole (1TTR), 4TTR, 5TTR, XTR. Detailed information on the analytes was provided in the Supplementary Material (Table S1). 5TTR and XTR were purchased from the Tokyo Chemical Industry (Shanghai, China), 1TTR was acquired from CNW (ANPEL Laboratory Technologies Inc., Shanghai, China), BTR and the instrument internal standard of HMB (hexamethylbenzene) were obtained from Dr. Ehrenstorfer (Augsburg, Germany), and 4TTR and BTR-d_4 were bought from Toronto Research Chemicals (Toronto, Canada). Individual stock solutions of the above compounds were prepared in acetone, and then a working standard solution was prepared by mixing the individual standard solutions and diluting in acetone to the required concentration. All solutions were stored at −20 °C.

Acetone, methanol, acetonitrile and dichloromethane in chromatographic grade solvents were purchased from Merck (Munchen, Germany). Sigma-Aldrich (St. Louis, MO, USA) supplied anhydrous sodium sulfate and silica gel (70–230 mesh). Both were of analysis purity grade and were heated at 400 °C for half an hour before use.

2.2. $PM_{2.5}$ sample collection and treatment

Sampling was carried out in the winter during November 2018 to January 2019. $PM_{2.5}$ samples were collected from Guangzhou (South China), Shanghai (East China) and Taiyuan (North China) (Fig. S1). The $PM_{2.5}$ sampling apparatuses were installed on the rooves of buildings at Shanxi University (Taiyuan), South China Normal University (Guangzhou) and Fudan University (Shanghai). No obvious sources of industrial pollution were found near the three sampling locations. Thus, the samples were considered to reflect the status of urban air particulate matter pollution. A total of 26 $PM_{2.5}$ samples were collected at the three locations for quantitative analysis. During the sampling period, temperature, pressure and humidity were recorded; detailed sampling information is listed in the Supplementary Material (Table S2). Ultrasonic extraction was used to extract BTRs from the

$PM_{2.5}$ samples. The pretreatment of samples was modified slightly from our previous publication (Liao et al., 2021).

2.3. Instrument method for BTRs quantitation

Separation and determination of the targets were performed on a Thermo TRACE™ 1300 gas chromatograph coupled to a TSQ 8000 Evo triple quadrupole mass spectrometer (Thermo Scientific, USA) with an electronic ionization (EI) source (GC-EI-MS/MS). A Thermo TG-5MS (5% phenyl-95% dimethylpolysiloxane; 30 m × 0.25 mm i.d.; 0.25 μm film thickness) capillary column (Thermo Scientific, USA) was used for the chromatographic separation. The detailed parameters of GC and MS conditions were supplied in the supplementary material.

2.4. Quality assurance and quality control (QA/QC)

Calibration curves, recoveries, precision and detection/quantification limits were considered to verify the performance of the analytical method. Calibration curves of BTRs were constructed with six or more points to determine the linear range and regression coefficient. The recoveries of five BTRs were determined by spiking a blank quartz filter sample with a mixed standard at a concentration of 1 $\mu g \cdot mL^{-1}$. A signal-to-noise ratio (S/N) of 3 and 10 was considered to correspond to the detection limit and limit of quantification, respectively (Ma et al., 2013; Van den Eede et al., 2011). As in our previous study (Liao et al., 2021), instrument detection limits (IDLs) were determined from the lowest standard concentrations, whereas method quantitation limits (MQLs) of each compound were calculated from the lowest concentration of $PM_{2.5}$ samples.

For quality control, program blanks and solvent blanks were used for the evaluation of potential background interference. A set amount of instrument internal standard hexamethylbenzene (HMB) was added to eliminate instrument errors in each sample before analysis. All glassware was heated at 450 °C for 5 h and then rinsed with dichloromethane (DCM) before use and between the sample treatment processes. The entire sample treatment process was carried out in a fume hood to avoid contamination.

2.5. Human exposure assessment

The health risks of exposure to pollutants may vary depending on the age group of the population. In this study, preliminary exposure risks were calculated for toddlers and adults in an outdoor environment. The concentration of BTRs in each region was used to estimate the daily intake $EDI_{\alpha p}$ (ng kg-bw^{-1} day^{-1}) of various human exposures according to Eq. (1):

$$EDI_{\alpha p} = \frac{C_{\alpha p} \times IR \times RR \times ABS_{\alpha} \times ET \times EF \times ED}{BW \times AT} \quad (1)$$

where $C_{\alpha p}$ is the environmental concentration of the target α at the sampling point p ($ng \cdot m^{-3}$), IR is the inspiratory rate ($m^3 \cdot h^{-1}$), RR is the retained air retention rate (%), ABS_{α} is the percentage of target α in the air absorbed into the blood (%), BW is the body weight (kg), ET and EF are the exposure time ($h \cdot d^{-1}$) and exposure frequency ($d \cdot yr^{-1}$), respectively, and ED is the duration of continuous exposure (years). AT is the average number of exposure days (days) calculated according to 365 $days \cdot yr^{-1}$ as AT = 365 × ED. Detailed parameter settings can be obtained in the Table S3.

2.6. Cardiotoxicity assessment

Toxicity screening on BTRs was examined by computational and experimental methods. At first, the theoretical LC_{50} values, cardiotoxicity and identified metabolites were predicted by using a ACD/Labs Percepta Platform (ACD/Labs, Toronto, Canada) and the OECD QSAR toolbox (www.qsartoolbox.org), which have been widely accepted and used in environmental science field. And then, neonatal rat cardiomyocytes (NRCMs) were used as a model for toxicity assessment in vitro. The methods used for NRCMs isolation and culture are detailed in the Supplementary Material. A MTT assay was used to screen the cytotoxicity of five BTRs according to the manufacturer's instructions (Beyotime Institute of Biotechnology, China). A concentration series of 100, 200, 500, 1000, 2000 and 4000 μM of each BTRs was prepared on a microwell plate to which were added NRCMs, and the plate was incubated for 48 h. The half lethal concentration (LC_{50}) of each substance was calculated based on the dose-response curve and used for toxicity assessment. The OECD QSAR Toolbox was used to predict the primary metabolites of 4TTR and 5TTR based on in vivo metabolism.

Based on the results of the MTT assay, 4TTR was found to be the most harmful substance of the five BTRs. To further investigate its toxic effects, an intracellular quantitative analysis, cell morphological analysis, intracellular reactive oxygen species (ROS) and apoptosis analysis, and mitochondrial function analysis after 48 h exposure. Detailed information of the methods was supplied in the Supplementary Material.

2.7. Western blot analysis

Mitochondrial apoptosis signaling pathway was examined by western blot assay. NRCMs were divided into control group, 4TTR (LC_{50}) group, 4TTR(LC_{50}) + *N*-acetylcysteine (NAC, 2 mM) group, respectively. After 48 h incubation, NRCMs were collected and the total protein extraction and western blot was performed as previously described (Qi et al., 2021). Briefly, 50 μg total proteins for each group were applied in this study and Anti-Bcl-2 antibody (SANTA CRUZ BIOTECHNOLOGY, INC), Anti-Bax antibody (Servicebio, Wuhan, China), Anti-Cytochrome C antibody (Servicebio), Anti-Caspase-9 antibody (Servicebio), Anti-Caspase-3 antibody (Servicebio), Anti-Cleaved Caspase-9 antibody (Cell Signaling Technology, CST, MA, USA), Anti-Cleaved Caspase-3 antibody (CST) and Anti-β-Actin antibody (CST) were used at 1:200, 1:500, 1:1000, 1:800, 1:500, 1:1000, 1:1000 and 1:1000, respectively. The targeted bands were analyzed using Image-Pro Plus 7.0 software (Media Cybernetics, Rockville, MD, USA).

2.8. Metabolomics analysis

2.8.1. Quenching of cells and metabolite extraction

NRCMs were exposed to 4TTR at the LC_{50} concentration to generate a treatment group and 0.1% dimethyl sulfoxide (DMSO) for a control group, with 9 replicates of each group. After 48 h exposure, the culture medium was removed, and the NRCMs were washed twice with phosphate-buffered saline (PBS), harvested by 0.5% trypsin digestion, and then collected and counted. The cells were rapidly quenched by addition of 1×10^7 cells to 5 volumes of 60% methanol supplemented with 0.85% (w/v) ammonium bicarbonate (pH 7.4) at −40 °C (Christopher et al., 2009; Sellick et al., 2011). Addition of the cells to the quenching solution increased the temperature by no more than 15 °C. The cell suspension was then centrifuged at 1000*g* for 1 min and the supernatant was removed.

The extraction method of metabolites was modified slightly from previous publications (Dietmair et al., 2010; Sellick et al., 2011). Each cell sample was resuspended in 500 μL extraction solution (80% methanol in water) and then incubated on ice for 10 min after vortex mixing for 30 s. The centrifuge tubes containing the samples were transferred to liquid nitrogen and snap-frozen for 10 min, then the samples were thawed and vortex mixing for another 30 s. This process was repeated once more to rupture the cells completely. Afterwards, the samples were centrifuged at 15000*g* for 5 min and the supernatant was collected and transferred to a fresh tube in an ice bath. Next, 500 μL of extraction solution was added to the pellet in the centrifuge tube and the above extraction process was repeated. The resulting extracts were combined and dried by a gentle stream of nitrogen. 120 μL of 50% methanol-

water was used to reconstitute the sample for HPLC analysis. A quality control (QC) sample was prepared by pooling 20 μL from each sample in the treatment and control groups.

2.8.2. Instrumental analysis

Untargeted metabolomics analysis was performed on an Agilent 1290 Infinity II ultrahigh performance liquid chromatograph, and a 6545 iFunnel quadrupole-time-of-flight (Q-TOF) mass spectrometer was coupled to the liquid system. A Waters HSS T3 column (2.1 mm × 100 mm, 1.8 μm) was used for metabolites separation. Targeted analysis of CoA and acetyl-CoA were analyzed by an Agilent 1260 Infinity II ultrahigh performance liquid chromatograph coupled to a 6470 Triple quadrupole mass spectrometer. A Waters XBridge BEH column (2.1 mm × 100 mm, 2.5 μm) was used for targets separation. The detailed parameters of UPLC and MS conditions were supplied in the Supplementary material.

2.9. Data analysis

One-way analysis of variance (one-way ANOVA) and principal component analysis (PCA) were performed to identify the contamination patterns of BTRs in $PM_{2.5}$ samples. Spearman's rank correlation analysis was used to evaluate possible relationships of BTRs detected at three sampling locations. Unpaired two-tailed *t*-test was applied to study the significant differences between exposure and control group. The variability and statistical significance of each variable were examined ($p \le 0.05$). Multivariate statistics (PLS-DA and OPLS-DA) were performed to identify potential makers for untargeted metabolomics. Details of the untargeted metabolomics analysis methods were provided in the Supplementary Material. All data analyses were performed using Graphpad Prism (version 8.1), SPSS (version 22.0), Origin (version 8.1) and SIMCA (version 14.1) for Windows.

3. Results and discussion

3.1. BTRs detection by GC-EI-MS/MS

Most previous studies have determined BTRs by liquid chromatography coupled to mass spectrometry or tandem mass spectrometry owing to their high water solubility and low volatility (Asimakopoulos et al., 2013a; Li et al., 2018; Wang et al., 2016). However, for the analysis of environmental samples, LC-MS/MS methods based on ESI are hampered by strong ion enhancement or inhibition, causing a strong matrix effect and making quantitative analysis difficult. Provided a suitable chromatographic column is selected, GC–MS/MS based on EI offers an effective and alternative detection method (Herrero et al., 2014). A fused-silica column coated with 5% diphenyl/95% polydimethylsiloxane has been applied for the separation of BTRs and shown to have a high separation efficiency (Liu et al., 2011; Loi et al., 2013; Naccarato et al., 2014). In the present study, a Thermo TG-5MS column (5% phenyl-95% dimethylpolysiloxane; 30 m × 0.25 mm i.d.; 0.25 μm film thickness) was used to separate the analytes. The long column length and gradient heating process enabled efficient separation of the substances. The separation of 4TTR and 5TTR allowed accurate quantitative analysis (Fig. 1a). We simultaneously optimized mass spectrum parameters such as quantitative, qualitative ions and collision energy of five BTRs (Table 1).

The standard curve linear range of BTRs was from 1 to 1000 $ng \cdot mL^{-1}$ except for BTR and BTR-d_4. All regression coefficients(R^2)exceeded 0.99 (Fig. S2), indicating a good linear relationship. In spiked blank quartz microfiber filters ($n = 6$), the recoveries of BTRs ranged from 66.3% (1TTR) to 89.2% (XTR), with an average recovery of 76.4% for BTRs and relative standard deviation of 4.44%, confirming the repeatability and reproducibility of the analytical method (Fig. 1b). BTRs were not detected in solvent blanks and procedural blanks. The IDLs and MQLs of the analytes were in the ranges 0.0020–1.2706 $ng \cdot mL^{-1}$ and 1.60–10.80 $pg \cdot m^{-3}$, respectively (Table S4). The IDLs and MQLs were reduced by more than 10 and 5 times in comparison with previous studies (Maceira et al., 2018; Nunez et al., 2020), respectively. The optimized method was efficient in real $PM_{2.5}$ samples (Fig. 1c).

3.2. Contamination profiles of BTRs in $PM_{2.5}$

The contamination profiles of $PM_{2.5}$-bound BTRs in three typical Chinese cities were identified using the optimized purification method. As shown in Table S5, BTRs were found with 100% detection ratio among three cities, indicating that they are widely distributed in the atmosphere as a consequence of their huge global production and application. A high mean concentration of ∑BTRs was found in Taiyuan (6.28 $ng \cdot m^{-3}$), followed by Guangzhou (1.99 $ng \cdot m^{-3}$) and Shanghai (1.53 $ng \cdot m^{-3}$), consistent with the $PM_{2.5}$ concentration in these three cities. In a previous study, the mean concentrations of PM_{10}-sourced ∑BTRs reported in Spain at Constantí (2.80 $ng \cdot m^{-3}$, range: 0.93–5.50 $ng \cdot m^{-3}$) and Tarragona harbour (2.20 $ng \cdot m^{-3}$, range: 0.69–4.10 $ng \cdot m^{-3}$) (Maceira et al., 2018) were above those at Guangzhou and Shanghai but significantly lower than that of Taiyuan. Nunez et al. also reported the mean concentrations of ∑BTRs associated with PM_{coarse} (range: 0.49–0.78 $ng \cdot m^{-3}$) and $PM_{2.5}$ (range: 0.26–0.49 $ng \cdot m^{-3}$) in the port of Tarragona (Nunez et al., 2020), which were far below the results of the present study. Our findings indicate that pollution contamination of ∑BTRs in China should be of concern, particularly in Taiyuan.

Significant differences were found in the environmental concentrations of BTR, 1TTR, 4TTR, 5TTR and XTR among the three cities. ($p < 0.05$, one-way ANOVA) (Fig. 2a). As shown in Fig. 2b and Fig. S3, BTR and 5TTR were the major pollutants among the BTRs, which accounted for more than 80% of the total BTRs concentration in the three cities. Wang et al. reported that BTR and TTR (4TTR and 5TTR) were the predominant compounds of total BTRs in indoor dust (Wang et al., 2013). BTR and TTR were also reported as predominant compounds among five BTRs detected in the vapor phase and bulk air in the USA (Xue et al., 2016). Not only were BTR and TTR the dominant compounds of ∑BTRs in the abovementioned air/particles but similar occurrences have been reported in other environmental or biological matrices, e.g., indoor dust from an e-waste dismantling area (Li et al., 2020), tap water, surface water and wastewater treatment plant effluents (Wang et al., 2016), wastewater (Asimakopoulos et al., 2013a), textiles (Liu et al., 2017), maternal urine and amniotic fluid (Li et al., 2018; Zhou et al., 2018), fish (Yao et al., 2018) and mollusks (Jia et al., 2019). Overall, we concluded that BTR and TTR are major components of total BTRs during production and application.

However, the distribution of BTR and 5TTR was strikingly different, showing opposite trends in the three cities. Mean concentrations of 5TTR in Taiyuan, Shanghai, Guangzhou were 5.32, 1.01, 0.67 $ng \cdot m^{-3}$, accounting for 85%, 66%, and 28% of the total BTRs concentration, respectively. According to previous research, 4TTR and 5TTR are widely used as aircraft deicing/anti-icing fluids (ADAFs), and hence their consumption increases in the winter, especially in regions of cold climate (Alotaibi et al., 2015; Steven et al., 2003; Steven et al., 2006; Walter et al., 2006). During sampling in the winter, the average temperature in Guangzhou, Shanghai and Taiyuan was 18.6 °C, 5.6 °C and −0.4 °C, respectively (Table S2). Owing to the low local temperatures, perhaps more ADAFs were applied to reduce freezing on roads and airports in Taiyuan. This might be an important reason for the high proportion of 5TTR in total BTRs and high ∑BTRs concentration in Taiyuan. The correlation between temperature and concentration of BTR and 5TTR was examined in more detail. Fig. 2c, d showed that there was a positive correlation between temperature and concentration of BTR and a negative correlation between temperature and concentration of 5TTR.

In order to further analyze the contamination pattern of BTRs in $PM_{2.5}$ samples, PCA was conducted. Before PCA analysis, Pareto scaling

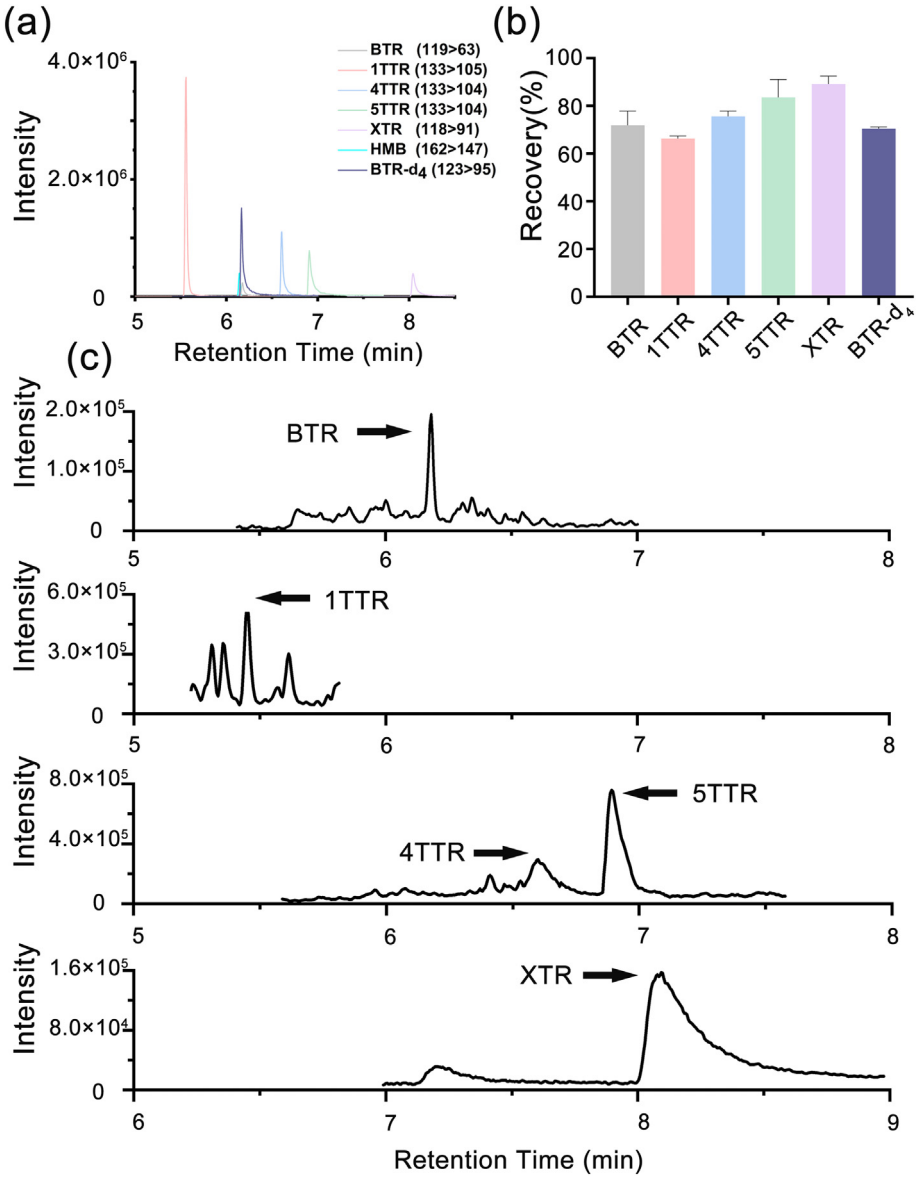

Fig. 1. Validation of the analytical methods used in the present study. (a) Extracted ion chromatograph of standard BTRs (1 μg·mL^{-1}). (b) Recoveries of spiked BTRs (1 μg·mL^{-1}). (c) Application of the optimized method in real $PM_{2.5}$ samples.

was performed on the concentration data to make it normally distributed. Two principal components, PC1 and PC2, were identified that explained 49.3% and 31% of the total variance, respectively. As shown in the two-dimensional PCA score chart in Fig. 2e, most data points were clearly separated according to the three different sampling locations, suggesting different sources for the BTRs. The corresponding PCA loading plot in Fig. 2f showed that 1TTR, 4TTR and 5TTR had similar high loadings on PC1, indicating source-related characteristics of 3 monomethyl benzotriazole derivatives. To further study the pollution source of BTRs in $PM_{2.5}$, Spearman's rank correlation was performed between the concentration of individual BTRs (Table S6). Positive correlations between the concentration of 1TTR and 4TTR ($R^2 = 0.895$, $p < 0.01$), 1TTR and 5TTR ($R^2 = 0.604$, $p < 0.01$), and 4TTR and 5TTR ($R^2 = 0.631$, $p < 0.01$) were found, in agreement with the PCA results, indicating a potential common source.

Table 1
Optimized quantitative/qualitative ions for analysis of BTRs by GC–MS/MS with the SRM mode.

Compound	Retention time (min)	Transition 1		Transition 2	
		Quantitative ion (*m*/*z*)	C.E.[c]	Qualitative ion (*m*/*z*)	C.E.[c]
BTR	6.20	119 > 63	25	119 > 52	20
1TTR	5.46	133 > 105	5	133 > 90	15
4TTR	6.59	133 > 104	10	133 > 78	10
5TTR	6.90	133 > 104	10	133 > 132	10
XTR	8.01	118 > 91	10	118 > 65	20
BTR-d_4[a]	6.17	123 > 95	5	123 > 67	15
HMB[b]	6.14	162 > 147	10	147 > 119	10

[a] Surrogate standard.
[b] Internal standard.
[c] Collision energy (eV).

3.3. Human exposure assessment

For comprehensive assessment of human exposure doses for BTRs, including BTRs concentrations, average body weight, average lifetime exposure period, inhalation rate and frequency were examined, as shown in Table S3. In the calculations, we assumed values (100%) for retention rate of inhaled air (RR) and the percentage of chemical absorbed

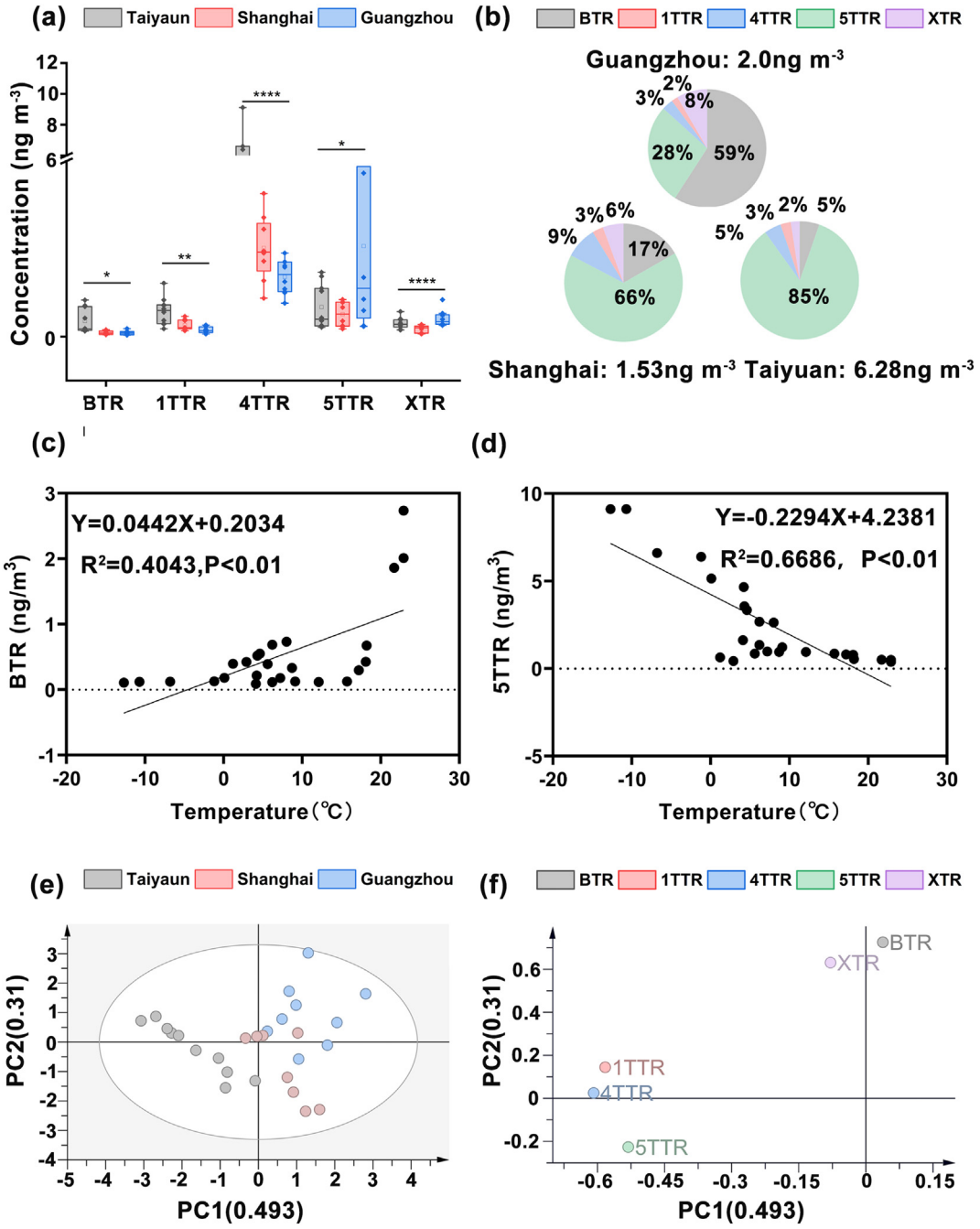

Fig. 2. Contamination profile of BTRs from urban $PM_{2.5}$. (a) Concentration of BTRs in Taiyuan, Guangzhou and Shanghai. (b) Relative abundance of BTRs in Taiyuan, Guangzhou and Shanghai. (c) Positive correlation of BTR concentration and temperature. (d) Negative correlation of 5TTR concentration and temperature. (e) Two-dimensional PCA score diagram. (f) Two-dimensional PCA loading diagram. $^{*}p < 0.05$, $^{**}p < 0.01$, $^{****}p < 0.001$.

into the bloodstream (ABS_{α}). Owing to the potentially different influences of BTRs exposure in different age groups, we calculated separate EDIs for toddlers and adults in the three cities. The mean and 95th percentile doses value represented a "typical" and "high" exposure scenario, respectively.

Table 2 shows that among the three cities, the mean EDI of individual BTRs ranged from 0.0157–1.9441 ng kg-bw^{-1} day^{-1} and 0.0055–0.6793 ng kg-bw^{-1} day^{-1} for toddlers and adults, respectively, whereas the 95th percentile EDI ranged from 0.0269–3.3276 ng kg-bw^{-1} day^{-1} for toddlers and 0.0094–1.1628 ng kg-bw^{-1} day^{-1} for adults. Thus, we found that the inhalation doses of BTRs in toddlers were 2 to 3 times higher than in adults. Similar results showing that inhalation doses decreased with age of population exposure to BTRs have been reported (Xue et al., 2016; Maceira et al., 2018). The mean EDI of ∑BTRs in Taiyuan (0.8018, 2.2946 ng kg-bw^{-1} day^{-1}) were 2 to 4 times higher than in Shanghai (0.1952, 1.281 ng kg-bw^{-1} day^{-1}) and Guangzhou (0.2549, 0.9961 ng kg-bw^{-1} day^{-1}) for adults and toddlers, which might be explained by the higher concentration of BTRs in Taiyuan. In general, the calculated values of EDI in the present study were of the same order of magnitude as those reported by Xue et al. for BTRs in indoor PM_{10} samples (0.91–3.23 ng kg-bw^{-1} day^{-1}) (Xue et al., 2016). Maceira et al. and Nunez et al. reported inhalation of particles of 0.28–0.99 ng kg-bw^{-1} day^{-1}

Table 2
Estimated daily intake (EDI, ng kg-bw^{-1} day^{-1}) of BTRs through inhalation of outdoor air ($PM_{2.5}$) in three Chinese cities for different age groups (toddlers and adults).

Compound	EDI(G)				EDI(S)				EDI(T)			
	Toddlers		Adults		Toddlers		Adults		Toddlers		Adults	
	Mean	95th percentile	Mean	95th percentile	Mean	95th percentile	Mean	95th percentile	Mean	95th percentile	Mean	95th percentile
BTR	0.3767	0.9063	0.1316	0.3167	0.0936	0.1510	0.0327	0.0528	0.1230	0.2603	0.0430	0.0906
1TTR	0.0157	0.0291	0.0055	0.0102	0.0167	0.0269	0.0058	0.0094	0.0652	0.1420	0.0228	0.0496
4TTR	0.0296	0.0473	0.0104	0.0165	0.0485	0.0798	0.0169	0.0279	0.1062	0.1910	0.0371	0.0667
5TTR	0.2440	0.3350	0.0853	0.1171	0.3687	0.5606	0.1288	0.1959	1.9441	3.3276	0.6793	1.1628
XTR	0.0632	0.0904	0.0221	0.0316	0.0317	0.0491	0.0110	0.0172	0.0561	0.0907	0.0196	0.0317
∑BTRs	0.7292	1.4081	0.2549	0.4921	0.5592	0.8674	0.1952	0.3032	2.2946	4.0116	0.8018	1.4014

and 0.03–0.49 ng kg-bw^{-1} day^{-1} in Spain, respectively, whereas a median EDI value of 0.28 ng kg-bw^{-1} day^{-1} has been reported for Chinese urban adult residents from indoor dust ingestion (Li et al., 2020; Maceira et al., 2018; Nunez et al., 2020). These values are close to the EDIs of Guangzhou and Shanghai but below those of Taiyuan. Thus, more attention should be paid to the BTRs exposure risk in Taiyuan.

3.4. Toxicity screening by using computational and experimental methods

To evaluate the toxicities of BTRs, the predicted LC_{50} and adverse effects on main biological systems were calculated with the ACD/Labs Percepta software, a widely used platform for toxicity prediction based on molecular's chemical structure. Gastrointestinal and circulation system (Blood and cardiovascular) were the main targeted sites affected by BTRs and minimum LC_{50} of BTR (6.6×10^{-4}, RI = 0.72) and 1TTR (2.4×10^{-4}, RI = 0.43) calculated by oral and subcutaneous injection, respectively (Table 3). It is noteworthy that 5TTR and 4TTR, having extremely similar structure and chemical and physical properties, such as log K_{OW} and log K_{OA}, were predicted with the same toxic ratio for different organ systems. However, the calculated values of LC_{50} for 5TTR and 4TTR were different in the oral and subcutaneous injection groups.

Although in silico prediction of chemical toxicity based on powerful databases have the advantages of fast, simple and low cost, considering the complexity and diversity of organisms as well as the huge variation in metabolic pathways, cell or animal-based experiments are still required to confirm the toxicity of chemical compounds. Therefore, NRCMs were used as a model for cardiovascular toxicity assessment in vitro. An initial cytotoxicity screening was conducted by MTT assay among five single BTRs. The LC_{50} values for BTR, 1TTR, 4TTR, 5TTR and XTR were calculated as 876.5 μM, 758.0 μM, 694.8 μM, 806.9 μM and 757.1 μM, respectively (Fig. 3a, b; Fig. S4). 4TTR demonstrated the highest cytotoxicity than other four benzotriazoles, which is consistent with previous study on zebrafish larvae reported by Damalas et al., 2018. Based on previous studies, the highest toxicity of 4TTR compared to benzotriazole and its other derivatives could be explained by 1) The internal concentration (C_{int}) of 4TTR in organisms was higher than that of BTR, 1TTR, XTR and was similar with 5TTR (Damalas et al., 2018; Brox et al., 2016). C_{int} can determine the toxicity to some extent (Escher et al., 2005). 2) 4TTR has more biochemical reactions (N—S, O—S coupling) in organisms, inducing more chemical stresses, which may be the reason why 4TTR is more toxic than 5TTR (Damalas et al., 2018). Subsequently, the potential metabolites of 4TTR and 5TTR were predicted by OECD QSAR Toolbox, simulating the primary process of rat in vivo metabolism of 4TTR and 5TTR (Table S7). Five primary metabolites were obtained by simulation of 4TTR, and only four metabolites were obtained by simulation of 5TTR. The simulation results were consistent with the conclusion of the above study and the results of our MTT experiments, suggesting 4TTR was the most toxic among five BTRs. Based on the present results, 4TTR was selected as a representative for further toxicity assessment at its LC_{50} value (694.8 μM).

3.5. 4TTR-induced mitochondrial-dependent apoptosis in NRCMs through ROS-mediated signaling pathways

At first, the concentration of 4TTR in NRCMs was monitored. After 48 h exposure 4TTR (694.8 μM), we detected 4TTR, and its mass concentration reached 31.65 ± 3.3 μg/g w/w in NRCMs (Fig. S5). This result suggested that 4TTR could pass through cell membranes and accumulate in NRCMs even with short-term exposure (48 h), which provided a prerequisite for exerting its toxic effects intracellularly. Liang et al. illustrated the neurotoxicity induced by BTRs in fish via neuroproteomics analysis (Liang et al., 2017). The results showed that BTRs exerted neurotoxicity to fish mainly by disturbing energy homeostasis in the central nervous system. Cardiac cells, belonging to the excitable cell type that similar to neural cells, are in great need of energy from mitochondria. Therefore, mitochondria play a key role in maintaining the cardiac function and deregulated mitochondrial activity has been implicated in the pathogenesis of several major cardiovascular diseases. As shown in Fig. 3c and d, the ratio of green/red fluorescence was markedly higher in the 4TTR treatment group compared to control group (3.60 ± 0.27 versus 2.21 ± 0.39, $p = 0.0058$), which indicated that exposure to 4TTR could induce the mitochondrial dysfunction under the condition of low mitochondrial membrane potential.

Dropped mitochondrial membrane potential, associating with the opening of the mitochondrial permeability pores and loss of the electrochemical gradient, is also an important indicator for the apoptotic

Table 3
Probability of health effects predicted using ACD/I-Lab 2.0.

Tissue		BTR	1TTR	4TTR	5TTR	XTR
Blood		0.41	0.14	0.39	0.39	0.37
Cardiovascular		0.17	0.03	0.14	0.14	0.11
Gastrointestinal		0.89	0.64	0.89	0.89	0.89
kidney		0.35	0.10	0.34	0.34	0.33
Liver		0.46	0.08	0.40	0.40	0.42
Lungs		0.17	0.16	0.15	0.15	0.12
LC_{50} (mg·L^{-1})	Rat/Intraperitoneal	6.6×10^{-4} (RI = 0.63)	2.4×10^{-4} (RI = 0.43)	6.5×10^{-4} (RI = 0.62)	7.0×10^{-4} (RI = 0.62)	6.1×10^{-4} (RI = 0.61)
	Rat/Oral	6.6×10^{-4} (RI = 0.72)	6.8×10^{-4} (RI = 0.50)	7.2×10^{-4} (RI = 0.70)	7.8×10^{-4} (RI = 0.70)	7.8×10^{-4} (RI = 0.70)

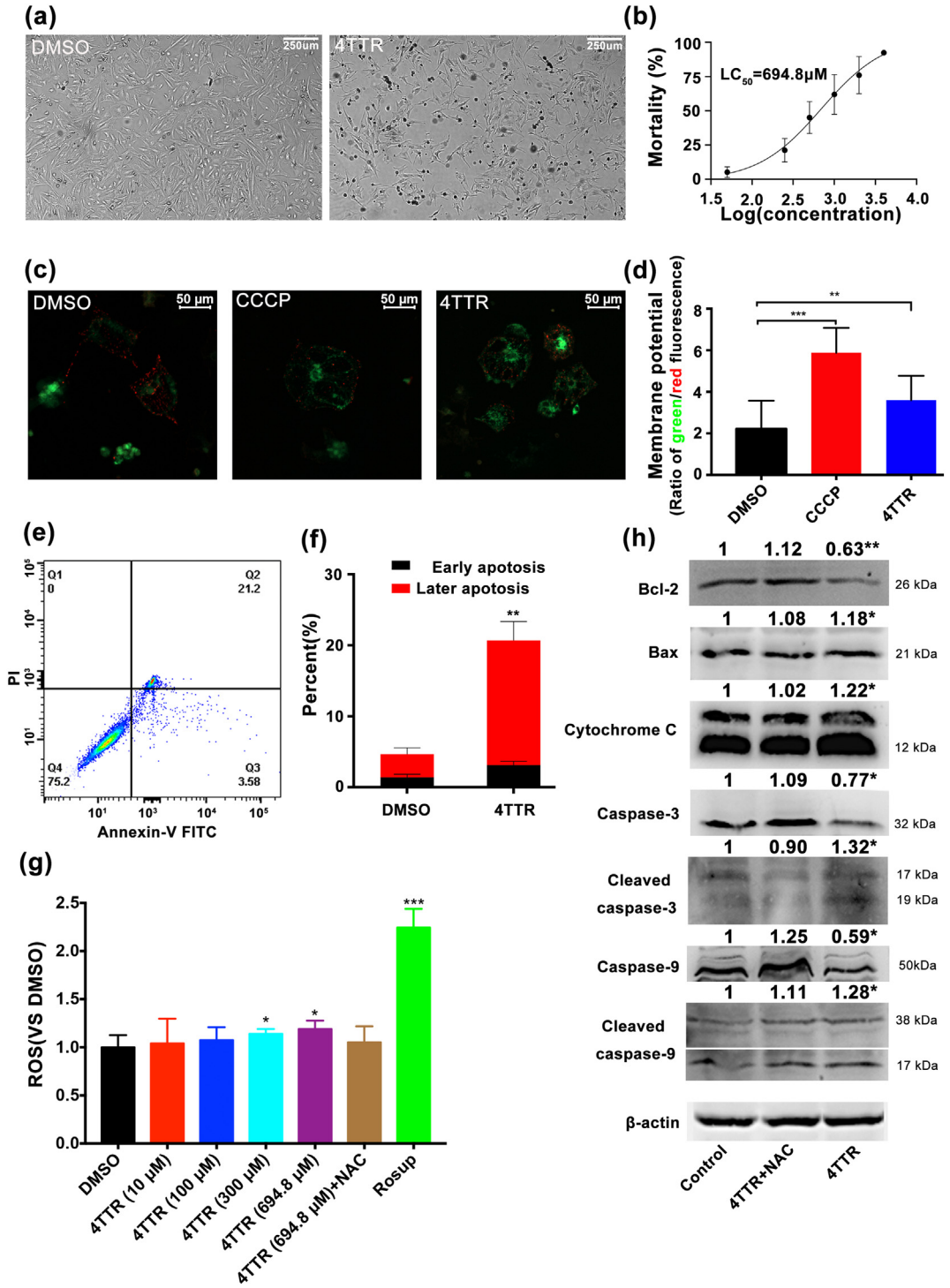

Fig. 3. Cytotoxic effects of 4TTR on NRCMs. (a) 10× magnification of cellular morphology of control group (DMSO) and treatment group (694.8 μM 4TTR). (b) Logarithmic-concentration versus response graph (MTT assay at 48 h). The NRCMs were cultured with various concentrations of 4TTR (100, 200, 500, 1000, 2000 and 4000 μM) for 48 h, and the LC_{50} concentration was 694.8 μM. (c) The mitochondrial membrane potential in control group (DMSO), treatment group (694.8 μM 4TTR) and positive control group (CCCP)was examined by red/green fluorescence with JC-1 staning in NRCMs. Scale bar: 50 μm. (d) Quantification of green to red JC-1 fluorescence intensity for DMSO, CCCP and 4TTR treated cells. At least15 cells from three independent experiments were selected for each group. (e) Apoptotic and necrotic populations were analyzed by FITC-annexin V and PI staining using flow cytometry. (f) The percentages of early apoptotic and late apoptotic/necrotic cells were calculated from three independent experiments. (g) Fold change of intracellular ROS after DMSO (Control), different concentrations of 4TTR, 4TTR(LC_{50}) + NAC (2 mM) and Rosup (Positive control) treatment. (h) 4TTR-induced alteration of the expression levels of Bcl-2, Bax, Caspase-3, Caspase-9, Cytochrome C, activated Caspase-3 and Caspase-9 were examined by western blotting analysis. β-actin was used as a housekeeping protein. The values are expressed as the mean ± SD of 3–7 independent experiments. $^{*}p < 0.05$, $^{**}p < 0.01$, $^{***}p < 0.005$ versus the control group.

process of cells. Subsequently, we further investigated whether 4TTR induced the apoptosis in NRCMs. After 48 h treatment with 4TTR (694.8 μM), the cell population of apoptosis had increased significantly in the treatment group (early: 3.13 ± 0.54 versus 1.39 ± 0.38, $p = 0.0085$; later: 17.58 ± 2.65 versus 3.3 ± 0.76, $p = 0.0023$) compared with those in the untreated controls (Fig. 3e and f). At the same time,

elevated intracellular ROS was detected in the 4TTR treatment group in a dose-dependent manner (Fig. 3g).

To investigate whether 4TTR-induced apoptosis was involved in the ROS-mediated mitochondrial apoptosis signaling pathway, the expression of a series of proteins in this pathway was detected after treatment with 4TTR and NAC, a ROS inhibitor. Compared with the control group, after treatment with 4TTR, the expression level of Bcl-2, Caspase-3 and Caspase-9 were decreased, but the expression of Bax, Cytochrome C, activated Caspase-3 and Caspase-9 were increased, which could be significantly blocked by NAC (Fig. 3h). Bcl-2 and Bax were the anti- and pro-apoptotic proteins in Bcl-2 family, which were the major regulators of apoptotic process. Caspases family were the executor of apoptosis process (Gross, 2016). In the present study, activated caspase cascade (Caspase 3 and 9), Bcl-2 family and released Cytochrome C reflected that elevated ROS levels mediated the activation of mitochondrial apoptosis pathway, which led to NRCMs' apoptosis.

These results revealed that the adverse efforts on cardiac cells may be involved in inducing the mitochondrial dysfunction, apoptosis and increasing the intracellular ROS. Previous experimental studies have emphasized that BTRs can have a significant adverse impact on the cells, tissues or organisms by inducing mitochondrial dysfunction, apoptosis and altering the ROS generation (Chen et al., 2020; Hemalatha et al., 2020; Zhang et al., 2020). Here, our results provided a deeper understanding of the potential risks of BTRs for the environment and especially for human health. At the same time, $PM_{2.5}$-triggered mitochondrial apoptosis has been reported by numerous studies (Liu et al., 2020; Liu et al., 2019; Jin et al., 2018). As a mixture, the overall toxicity of total $PM_{2.5}$ should be a combination of its components (Qi et al., 2020). Thus, it is believed that $PM_{2.5}$-bound BTRs may be an important effector for $PM_{2.5}$-triggered mitochondrial apoptosis.

3.6. 4TTR disturbed the mitochondrial energy metabolism in NRCMs by reducing coenzyme A synthesis and pyruvate metabolism

NRCM samples were analyzed by UPLC Q-TOF-MS to identify significantly changed metabolites, SIMCA software (version 14.1) was used for multivariate statistical analysis. In the PLS-DA diagram (Fig. S6a), the data points of the 4TTR, DMSO and QC groups were obviously separated and the data points of the QC group were densely clustered, which not only indicated that the source properties of the samples after exposure were different but also verified the stability of the instrument in both the positive and negative ion modes. To more accurately screen for differential metabolites, we performed OPLS-DA analysis (Fig. S6b) on the data of the 4TTR and DMSO groups by calculating the VIP value of each fragment ion. The permutation validation of PLS-DA and OPLS-DA ($n = 200$) indicated that the mode had no overfitting and high reliability (Fig. S6c, S6d). All the differential endogenous metabolites meeting the conditions VIP > 1.0 and $p < 0.05$ were examined by secondary mass spectrometry analysis. A total of 19 metabolites (Table 4) were identified from the HMDB and METLIN databases and subjected to KEGG metabolic pathway enrichment analysis.

As shown in Fig. S7, the 19 identified metabolites changed significantly between the 4TTR and DMSO groups: expression of 7 metabolites was upregulated, whereas the other 12 were downregulated in the 4TTR group. According to the type of metabolite and degree to which it was upregulated or downregulated, corresponding metabolic pathways were identified. Among the possible metabolic pathways (Fig. 4a), coenzyme A (CoA) biosynthesis was severely affected. CoA is a ubiquitous cofactor in all living cells and plays a vital role in many biochemical reactions, including the breakdown of sugars, oxidation of fatty acids, breakdown of amino acids, degradation of pyruvate and activation of the tricarboxylic acid (TCA) cycle, which provides 90% of the body's energy needs for life (Abo Alrob and Lopaschuk, 2014; Bakovi et al., 2021; Leonardi et al., 2005). In the present study, the concentration of L-cysteine, dephospho-CoA, and pantetheine 4′-phosphate were decreased significantly in the 4TTR group. These three compounds are intermediates in the biosynthesis of CoA. Simultaneously, the concentration of pyruvic acid was increased in the 4TTR group. It was speculated that the degradation of pyruvate might be affected, leading to reduced acetyl-CoA biosynthesis, which in turn would affect the whole TCA cycle of NRCMs. For the miss of CoA and acetyl-CoA in the untargeted metabolomics profiling, we then analyzed the concentrations of CoA and acetyl-CoA in NRCMs by UPLC-MS/MS. Compared with control groups, CoA and acetyl-CoA significantly decreased (Fig. S8). We concluded that 4TTR exposure reduced the synthesis of

Table 4
Differential metabolites identified in NRCMs after 48 h exposure to 4TTR.

Compound (ion mode)	RT (min)	Formula	HMDB ID	*m/z* observed	*m/z* theoretical	Delta[a] (ppm)	VIP[b]	*p* value	Fold change
L-Cysteine (+)	6.42	$C_3H_7NO_2S$	HMDB0000574	122.0268	122.0270	1.6	1.25	****	0.61
Pantetheine 4′-phosphate (+)	15.27	$C_{11}H_{23}N_2O_7PS$	HMDB0001416	358.0963	358.0964	0.3	2.08	****	0.64
Glycyltyrosine (+)	4.78	$C_{11}H_{14}N_2O_4$	HMDB0028853	239.1025	239.1026	0.4	2.05	****	0.67
Tetraethylene glycol (+)	7.81	$C_8H_{18}O_5$	HMDB0094708	195.1218	195.1227	4.6	1.31	****	1.48
Dephospho-CoA (+)	18.21	$C_{21}H_{35}N_7O_{13}P_2S$	HMDB0001373	688.5189	688.5180	−1.3	1.16	*	0.49
Tryptophan (+)	0.96	$C_{11}H_{12}N_2O_2$	HMDB0030396	227.0796	227.0796	0	1.12	****	0.58
Cuscohygrine (+)	14.47	$C_{13}H_{24}N_2O$	HMDB0030290	225.1961	225.1961	0	2.38	**	1.27
Histidyltyrosine (+)	3.93	$C_{15}H_{18}N_4O_4$	HMDB0028897	319.1404	319.1401	−0.9	1.07	***	0.48
Phytyl diphosphate (+)	8.33	$C_{20}H_{42}O_7P_2$	HMDB0011116	457.2484	457.2479	−1.1	2.57	****	0.63
L-Tyrosine (+)	0.95	$C_9H_{11}NO_3$	HMDB0000158	182.0812	182.0812	0	1.02	****	1.30
Docosanamide (+)	18.29	$C_{22}H_{45}NO$	HMDB0000583	340.3571	340.3574	0.9	2.34	****	1.21
Pyrrhoxanthinol (+)	9.55	$C_{37}H_{46}O_5$	HMDB0035696	571.3436	571.3418	−3	1.52	****	0.57
5-Aminoimidazole ribonucleotide (+)	0.92	$C_8H_{14}N_3O_7P$	HMDB0001235	296.0661	296.0642	−6	1.18	****	1.64
Alanylphenylalanine (+)	8.68	$C_{12}H_{16}N_2O_3$	HMDB0028694	237.1233	237.1234	0.4	1.22	****	0.65
Dihomo-gamma-linolenoylethanolamide (−)	18.76	$C_{22}H_{39}NO_2$	HMDB0013625	348.2894	348.2908	4	2.28	***	0.64
Portensterol (−)	19.35	$C_{28}H_{44}O_2$	HMDB0034331	411.3299	411.3269	−7.3	11.12	*	0.70
Pyruvic acid (−)	3.43	$C_3H_4O_3$	HMDB0000243	87.0087	87.0088	1.1	1.84	****	1.52
L-Glutamine (−)	0.80	$C_5H_{10}N_2O_3$	HMDB0003423	145.0617	145.0619	1.4	2.33	***	1.66
Creatine (−)	2.56	$C_4H_9N_3O_2$	HMDB0000064	130.0624	130.0622	−1.5	1.30	****	0.52

[a] Delta = ((*m/z* theoretical) − (*m/z* observed)) / (*m/z* observed) * 10^6.
[b] Variable importance in projection.
* $p < 0.05$.
** $p < 0.01$.
*** $p < 0.005$.
**** $p < 0.001$.

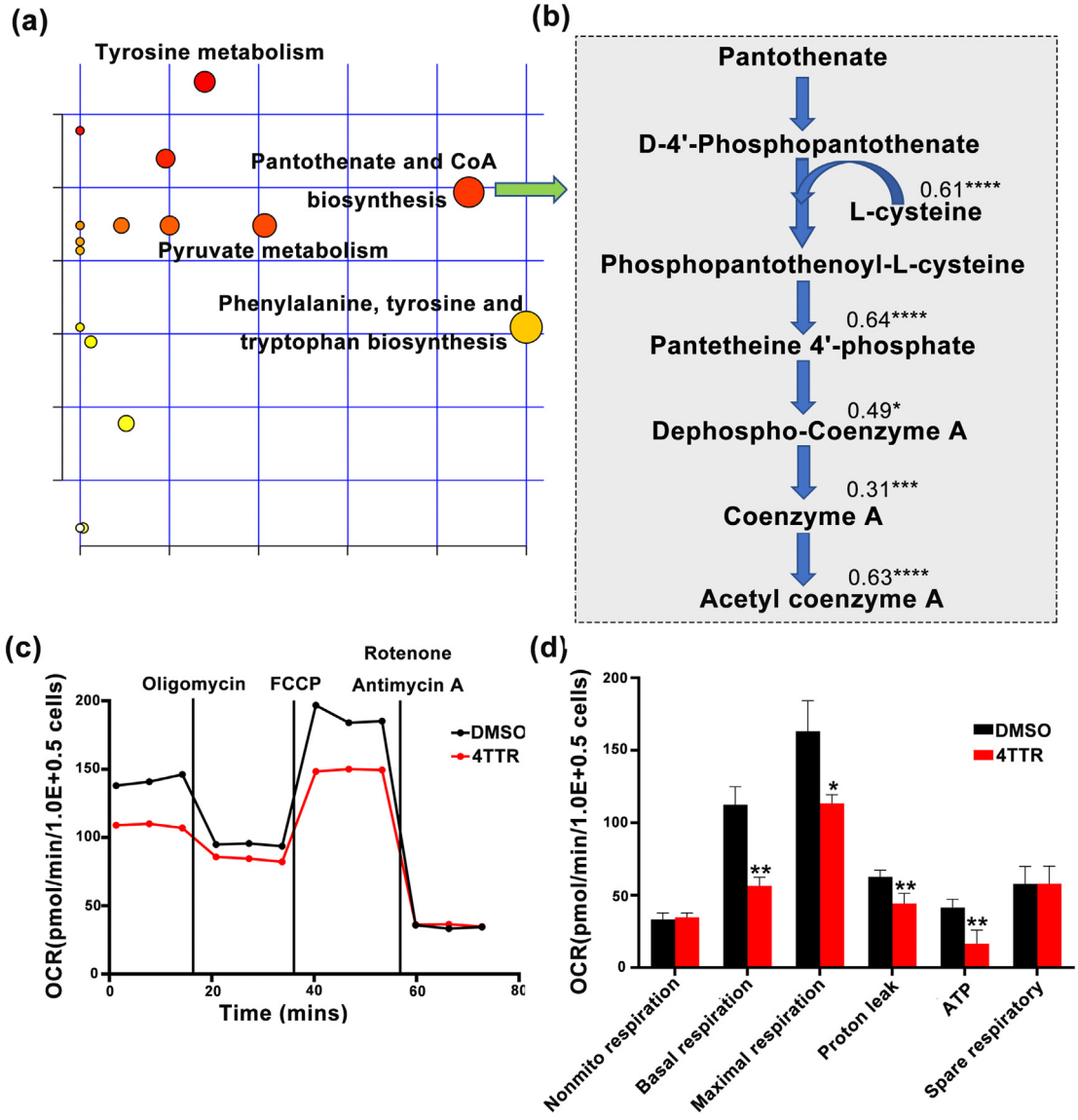

Fig. 4. Metabolomicsand mitochondrial function analysis. (a) Pathway analysis of metabolomics data in NRCMs after 4TTR exposure (694.8 μM). (b) Pantothenate and coenzyme A synthesis pathway and acetyl-CoA in NRCMs were analyzed by metabolomics. (c) showed the mitochondrial energy production function in NRCMs after 48 h of treatment with 4TTR (694.8 μM) as compared to control. (d) Statistical changes of each value in the process of mitochondrial energy production. Values are mean ± SD of 3–7 independent experiments. $^{*}P < 0.05$, $^{**}P < 0.01$ versus the control group.

CoA and further affected the synthesis of its acetyl product acetyl-CoA (Fig. 4b). In our study, the mitochondrial energy metabolism in NRCMs was also examined by Seahorse XF Assay. Treatment with 4TTR for 48 h obviously decreased the mitochondrial respiration function and ATP production measured as oxygen consumption rate in NRCMs (Fig. 4c, d). These results confirmed that 4TTR has significant potential to exert harmful biologic effects in cardiac cells by disturbing the energy metabolism.

In the heart, any small change of cardiac energy metabolism can lead to serious disease, including myocardial infarction, heart failure, hypertrophy and other problems after long accumulation (Lopaschuk et al., 2007; Tuomainen and Tavi, 2017). In addition, several other metabolic pathways were slightly affected, including tyrosine metabolism and phenylalanine, tyrosine and tryptophan biosynthesis pathways. In conclusion, acute exposure to 4TTR led to a decrease in the concentration of intracellular mediators involved in CoA synthesis in NRCMs, inability to synthesize coenzyme A and its acetylated product acetyl coenzyme-A, inhibition of pyruvate degradation, and effects on energy metabolism in cardiomyocytes.

4. Conclusions

This study was designed to explore the contamination profiles and exposure risk of $PM_{2.5}$-bound BTRs in three typical Chinese cities (Taiyuan, Shanghai and Guangzhou). The concentration of ∑BTRs in Taiyuan was two times higher than that in Shanghai and Guangzhou, consistent with the $PM_{2.5}$ concentration in the three cities. The distribution of each BTRs varied, with BTR and 5TTR being the dominant compounds among five BTRs studied in the three cities. In addition, 4TTR demonstrated the highest cytotoxicity of the five benzotriazoles by using computational and experimental methods. We further investigated the toxic effects of 4TTR using an NRCM model in vitro. After exposure to 4TTR, increased apoptosis was observed and metabolic pathways such as CoA synthesis and pyruvate metabolism were affected, which could block energy metabolism in cardiomyocytes. Therefore, long-term exposure to 4TTR may lead to serious cardiovascular disease. Thus, overall, more attention should be paid to the contamination profiles of $PM_{2.5}$-bound BTRs and exposure risk, especially in rapidly developing cities such as Taiyuan.

CRediT authorship contribution statement

Chun Yang: Conceptualization, Investigation, Formal analysis, Writing – original draft, Writing – review & editing. **Shiyao He:** Investigation, Data curation. **Shimin Lu:** Investigation, Data curation. **Xiaoliang Liao:** Conceptualization, Investigation. **Yuanyuan Song:** Investigation, Data curation. **Zhi-Feng Chen:** Investigation, Data curation. **Guoxia Zhang:** Investigation. **Ruijin Li:** Writing – review & editing, Supervision. **Chuan Dong:** Conceptualization, Supervision. **Zenghua Qi:** Conceptualization, Investigation, Formal analysis, Data curation, Writing – original draft, Writing – review & editing, Supervision. **Zongwei Cai:** Conceptualization, Writing – original draft, Writing – review & editing, Supervision.

Declaration of competing interest

The authors declare that they have no known competing financial interests or personal relationships that could have appeared to influence the work reported in this paper.

Acknowledgements

This work was supported by the National Natural Science Foundation of China (21806025 and 91843301), the Natural Science Foundation of Guangdong Province (2019A1515011294), the General Research Fund from Hong Kong Research Grants Council (12303320), the Science and Technology Planning Project of Guangdong Province (2020B1212030008) and the National Key Research and Development Project (2019YFC1804604), National College Students Innovation and Entrepreneurship Training Program (S202011845181).

Appendix A. Supplementary data

Supplementary data to this article can be found online at https://doi.org/10.1016/j.scitotenv.2021.151132.

References

Abo Alrob, O., Lopaschuk, G., 2014. Role of CoA and acetyl-CoA in regulating cardiac fatty acid and glucose oxidation. Biochem. Soc. Trans. 42 (4), 1043–1051.
Alotaibi, M.D., McKinley, A.J., Patterson, B.M., Reeder, A.Y., 2015. Benzotriazoles in the aquatic environment: a review of their occurrence, toxicity, degradation and analysis. Water Air Soil Pollut. 226, 1–20.
Amrani, A., Rosenberg, Y.O., Meshoulam, A., Said-Ahmad, W., Turich, C., Luu, N., Jacksier, T., Stankiewicz, A., Feinstein, S., Shurki, A., 2019. Sulfur isotopic composition of gas-phase organic sulfur compounds provides insights into the thermal maturation of organic-rich rocks. Geochim. Cosmochim. Acta 259, 91–108.
Asimakopoulos, A.G., Ajibola, A., Kannan, K., Thomaidis, N.S., 2013a. Occurrence and removal efficiencies of benzotriazoles and benzothiazoles in a wastewater treatment plant in Greece. Sci. Total Environ. 452–453, 163–171.
Asimakopoulos, A.G., Bletsou, A.A., Wu, Q., Thomaidis, N.S., Kannan, K., 2013b. Determination of benzotriazoles and benzothiazoles in human urine by liquid chromatography-tandem mass spectrometry. Anal. Chem. 85, 441–448.
Asimakopoulos, A.G., Wang, L., Thomaidis, N.S., Kannan, K., 2013c. Benzotriazoles and benzothiazoles in human urine from several countries: a perspective on occurrence, biotransformation, and human exposure. Environ. Int. 59, 274–281.
Bakovi, J., Martínez, D., Nikolaou, S., Yu, B., Gout, I., 2021. Regulation of the CoA biosynthetic complex assembly in mammalian cells. Int. J. Mol. Sci. 22 (3), 1131.
Brox, S., Seiwert, B., Kuster, E., Reemtsma, T., 2016. Toxicokinetics of polar chemicals in zebrafish embryo (Danio rerio): influence of physicochemical properties and of biological processes. Environ. Sci. Technol. 50, 10264–10272.
Chen, X., Zhou, Y., Hu, C., Xia, W., Xu, S., Cai, Z., Li, Y., 2020. Prenatal exposure to benzotriazoles and benzothiazoles and cord blood mitochondrial DNA copy number: a prospective investigation. Environ. Int. 143, 105920.
Christopher, S.A., Hansen, R., Maqsood, A.R., Dunn, W.B., Stephens, G.M., Goodacre, R., Dickson, A.J., 2009. Effective quenching processes for physiologically valid metabolite profiling of suspension cultured mammalian cells. Anal. Chem. 81, 174–183.
Damalas, D.E., Bletsou, A.A., Agalou, A., Beis, D., Thomaidis, N.S., 2018. Assessment of the acute toxicity, uptake and biotransformation potential of benzotriazoles in zebrafish (Danio rerio) larvae combining HILIC- with RPLC-HRMS for high-throughput identification. Environ. Sci. Technol. 52, 6023–6031.
Dietmair, S., Timmins, N.E., Gray, P.P., Nielsen, L.K., Kromer, J.O., 2010. Towards quantitative metabolomics of mammalian cells: development of a metabolite extraction protocol. Anal. Biochem. 404, 155–164.
Escher, B., Hermens, J., Schwarzenbach, R., 2005. International workshop. Internal exposure–linking bioavailability to effects. Environ. Sci. Pollut. Res. 12, 57–60.
Fent, K., Chew, G., Li, J., Gomez, E., 2014. Benzotriazole UV-stabilizers and benzotriazole: antiandrogenic activity in vitro and activation of aryl hydrocarbon receptor pathway in zebrafish eleuthero-embryos. Sci. Total Environ. 482–483, 125–136.
Garcia-Gomez, D., Bregy, L., Nussbaumer-Ochsner, Y., Gaisl, T., Kohler, M., Zenobi, R., 2015. Detection and quantification of benzothiazoles in exhaled breath and exhaled breath condensate by real-time secondary electrospray ionization-high-resolution mass spectrometry and ultra-high performance liquid chromatography. Environ. Sci. Technol. 49, 12519–12524.
Gross, A., 2016. BCL-2 family proteins as regulators of mitochondria metabolism. Biochim. Biophys. Acta 1857, 1243–1246.
Hart, D.S., Davis, L.C., Erickson, L.E., Callender, T.M., 2004. Sorption and partitioning parameters of benzotriazole compounds. Microchem. J. 77, 9–17.
Hemalatha, D., Rangasamy, B., Nataraj, B., Maharajan, K., Narayanasamy, A., Ramesh, M., 2020. Transcriptional, biochemical and histological alterations in adult zebrafish (Danio rerio) exposed to benzotriazole ultraviolet stabilizer-328. Sci. Total Environ. 739, 139851.
Herrero, P., Borrull, F., Pocurull, E., Marcé, R.M., 2014. An overview of analytical methods and occurrence of benzotriazoles, benzothiazoles and benzenesulfonamides in the environment. Trends Analyt Chem. 62, 46–55.
Janna, H., Scrimshaw, M.D., Williams, R.J., Churchley, J., Sumpter, J.P., 2011. From dishwasher to tap? Xenobiotic substances benzotriazole and tolyltriazole in the environment. Environ. Sci. Technol. 45, 3858–3864.
Jia, J., Zhu, Q., Liu, N., Liao, C., Jiang, G., 2019. Occurrence of and human exposure to benzothiazoles and benzotriazoles in mollusks in the Bohai SeaChina. 130, 104925.
Jin, X., Xue, B., Zhou, Q., Su, R., Li, Z., 2018. Mitochondrial damage mediated by ROS incurs bronchial epithelial cell apoptosis upon ambient PM2.5 exposure. J Toxicol Sci. 43 (2), 101–111.
Leonardi, R., Zhang, Y.M., Rock, C.O., Jackowski, S., 2005. Coenzyme a: back in action. Prog. Lipid Res. 44, 125–153.
Li, X., Wang, L., Asimakopoulos, A.G., Sun, H., Zhao, Z., Zhang, J., Zhang, L., Wang, Q., 2018. Benzotriazoles and benzothiazoles in paired maternal urine and amniotic fluid samples from TianjinChina. 199, 524–530.
Li, W., Li, J., Deng, M., Pan, Y., Zeng, L., 2020. Benzotriazoles and benzothiazoles prevail in indoor dust from an E-waste dismantling area in South China: elevated concentrations and implication for human exposure. Sci. Total Environ. 723, 137979.
Liang, X., Zha, J., Martyniuk, C.J., Wang, Z., Zhao, J., 2017. Histopathological and proteomic responses in male Chinese rare minnow (Gobiocypris rarus) indicate hepatotoxicity following benzotriazole exposure. Environ. Pollut. 229, 459–469.
Liao, X., Zou, T., Chen, M., Song, Y., Yang, C., Qiu, B., Chen, Z.F., Tsang, S.Y., Qi, Z., Cai, Z., 2021. Contamination profiles and health impact of benzothiazole and its derivatives in PM2.5 in typical chinese cities. Sci. Total Environ. 755, 142617.
Liu, Y.S., Ying, G.G., Shareef, A., Kookana, R.S., 2011. Simultaneous determination of benzotriazoles and ultraviolet filters in ground water, effluent and biosolid samples using gas chromatography-tandem mass spectrometry. J. Chromatogr. A 1218, 5328–5335.
Liu, W., Xue, J., Kannan, K., 2017. Occurrence of and exposure to benzothiazoles and benzotriazoles from textiles and infant clothing. Sci. Total Environ. 592, 91–96.
Liu, J., Liang, S., Du, Z., Zhang, J., Sun, B., Zhao, T., Yang, X., Shi, Y., Duan, J., Sun, Z., 2019. PM2.5 aggravates the lipid accumulation, mitochondrial damage and apoptosis in macrophage foam cells. Environ. Pollut. 249, 482–490.
Liu, X., Zhao, X., Li, X., Lv, S., Ma, R., Qi, Y., Abulikemu, A., Duan, H., Guo, C., Li, Y., Sun, Z., 2020. PM2.5 triggered apoptosis in lung epithelial cells through the mitochondrial apoptotic way mediated by a ROS-DRP1-mitochondrial fission axis. J. Hazard. Mater. 397, 122608.
Loi, C.H., Busetti, F., Linge, K.L., Joll, C.A., 2013. Development of a solid-phase extraction liquid chromatography tandem mass spectrometry method for benzotriazoles and benzothiazoles in wastewater and recycled water. J. Chromatogr. A 1299, 48–57.
Loos, R., Gawlik, B.M., Locoro, G., Rimaviciute, E., Contini, S., Bidoglio, G., 2009. EU-wide survey of polar organic persistent pollutants in European river waters. Environ. Pollut. 157, 561–568.
Lopaschuk, G.D., Folmes, C.D., Stanley, W.C., 2007. Cardiac energy metabolism in obesity. Circ. Res. 101, 335–347.
Ma, Y., Cui, K., Zeng, F., Wen, J., Liu, H., Zhu, F., Ouyang, G., Luan, T., Zeng, Z., 2013. Microwave-assisted extraction combined with gel permeation chromatography and silica gel cleanup followed by gas chromatography-mass spectrometry for the determination of organophosphorus flame retardants and plasticizers in biological samples. Anal. Chim. Acta 786, 47–53.
Maceira, A., Marce, R.M., Borrull, F., 2018. Occurrence of benzothiazole, benzotriazole and benzenesulfonamide derivates in outdoor air particulate matter samples and human exposure assessment. Chemosphere 193, 557–566.
McNeill, K.S., Cancilla, D.A., 2009. Detection of triazole deicing additives in soil samples from airports with low, mid, and large volume aircraft deicing activities. Bull. Environ. Contam. Toxicol. 82, 265–269.
Naccarato, A., Gionfriddo, E., Sindona, G., Tagarelli, A., 2014. Simultaneous determination of benzothiazoles, benzotriazoles and benzosulfonamides by solid phase microextraction-gas chromatography-triple quadrupole mass spectrometry in environmental aqueous matrices and human urine. J. Chromatogr. A 1338, 164–173.
Nunez, A., Vallecillos, L., Marce, R.M., Borrull, F., 2020. Occurrence and risk assessment of benzothiazole, benzotriazole and benzenesulfonamide derivatives in airborne particulate matter from an industrial area in Spain. Sci. Total Environ. 708, 135065.
Qi, Z., Zhang, Y., Chen, Z.F., Yang, C., Song, Y., Liao, X., Li, W., Tsang, S.Y., Liu, G., Cai, Z., 2020. Chemical identity and cardiovascular toxicity of hydrophobic organic components in PM2.5. Ecotoxicol. Environ. Saf. 201, 110827.
Pena, M.T., Vecino-Bello, X., Casais, M.C., Mejuto, M.C., Cela, R., 2012. Optimization of a dispersive liquid–liquid microextraction method for the analysis of benzotriazoles and benzothiazoles in water samples. Anal. Bioanal. Chem. 402, 1679–1695.

Qi, Z., Yang, C., Liao, X., Song, Y., Zhao, L., Liang, X., Su, Y., Chen, Z.F., Li, R., Dong, C., Cai, Z., 2021. Taurine reduction associated with heart dysfunction after real-world PM2.5 exposure in aged mice. Sci. Total Environ. 782, 146866.

Sellick, C.A., Hansen, R., Stephens, G.M., Goodacre, R., Dickson, A.J., 2011. Metabolite extraction from suspension-cultured mammalian cells for global metabolite profiling. Nat. Protoc. 6, 1241–1249.

Shi, Z.Q., Liu, Y.S., Xiong, Q., Cai, W.W., Ying, G.G., 2019. Occurrence, toxicity and transformation of six typical benzotriazoles in the environment: a review. Sci. Total Environ. 661, 407–421.

Steven, C.R., Daniel, Z.H., Jennifer, F.A., Devon, C.A., 2003. Nonylphenol ethoxylates and other additives in aircraft deicers, antiicers, and waters receiving airport runoff. Environ. Sci. Technol. 37, 4031–4037.

Steven, C.R., Steven, G.W., Loyo-Rosales, J.E., Rice, C.P., 2006. Aquatic toxicity of nine aircraft deicer and anti-icer formulations and relative toxicity of additive package ingredients alkylphenol ethoxylates and 4,5-Methyl-1H-benzotriazoles. Environ. Sci. Technol. 40, 7409–7415.

Trabalon, L., Nadal, M., Borrull, F., Pocurull, E., 2017. Determination of benzothiazoles in seafood species by subcritical water extraction followed by solid-phase microextraction-gas chromatography-tandem mass spectrometry: estimating the dietary intake. Anal. Bioanal. Chem. 409, 5513–5522.

Tuomainen, T., Tavi, P., 2017. The role of cardiac energy metabolism in cardiac hypertrophy and failure. Exp. Cell Res. 360, 12–18.

Turpin, B.J., Lim, H.-J., 2001. Species contributions to PM2.5 mass concentrations: revisiting common assumptions for estimating organic mass. Aerosol Sci. Technol. 35, 602–610.

Van den Eede, N., Dirtu, A.C., Neels, H., Covaci, A., 2011. Analytical developments and preliminary assessment of human exposure to organophosphate flame retardants from indoor dust. Environ. Int. 37, 454–461.

Walter, G., Christian, S., Hans-Peter, K.E., 2006. Benzotriazole and tolyltriazole as aquatic contaminants. 1. input and occurrence in rivers and lakes. Environ. Sci. Technol. 40, 7186–7192.

Wan, Y., Xue, J., Kannan, K., 2016. Benzothiazoles in indoor air from Albany, New York, USA, and its implications for inhalation exposure. J. Hazard. Mater. 311, 37–42.

Wang, L., Asimakopoulos, A.G., Moon, H.B., Nakata, H., Kannan, K., 2013. Benzotriazole, benzothiazole, and benzophenone compounds in indoor dust from the United States and east Asian countries. Environ. Sci. Technol. 47, 4752–4759.

Wang, L., Asimakopoulos, A.G., Kannan, K., 2015. Accumulation of 19 environmental phenolic and xenobiotic heterocyclic aromatic compounds in human adipose tissue. Environ. Int. 78, 45–50.

Wang, L., Zhang, J., Sun, H., Zhou, Q., 2016. Widespread occurrence of benzotriazoles and benzothiazoles in tap water: influencing factors and contribution to human exposure. Environ. Sci. Technol. 50, 2709–2717.

Wang, Y., Dai, C., Zhou, C., Li, W., Qian, Y., Wen, J., Wang, Y., Han, B., Ma, J., Xu, J., Fu, Z., Ruan, H., Tong, H., Jia, X., 2017. Benzotriazole enhances cell invasive potency in endometrial carcinoma through CTBP1-mediated epithelial-mesenchymal transition. Cell. Physiol. Biochem. 44, 2357–2367.

Weiss, S., Jakobs, J., Reemtsma, T., 2006. Discharge of three benzotriazole corrosion inhibitors with municipal wastewater and improvements by membrane bioreactor treatment and ozonation. Environ. Sci. Technol. 40, 7193–7199.

Wu, X., Vu, T.V., Shi, Z., Harrison, R.M., Liu, D., Cen, K., 2018. Characterization and source apportionment of carbonaceous PM2.5 particles in China - a review. Atmos. Environ. 189, 187–212.

Xue, J., Wan, Y., Kannan, K., 2016. Occurrence of benzotriazoles (BTRs) in indoor air from Albany, New York, USA, and its implications for inhalation exposure. Toxicol. Environ. Chem. 99, 402–414.

Yao, L., Zhao, J.L., Liu, Y.S., Zhang, Q.Q., Jiang, Y.X., Liu, S., Liu, W.R., Yang, Y.Y., Ying, G.G., 2018. Personal care products in wild fish in two main Chinese rivers: bioaccumulation potential and human health risks. Sci. Total Environ. 621, 1093–1102.

Zhang, Z., Ren, N., Li, Y.F., Kunisue, T., Gao, D., Kannan, K., 2011. Determination of benzotriazole and benzophenone UV filters in sediment and sewage sludge. Environ. Sci. Technol. 45, 3909–3916.

Zhang, H., Xing, Y., Ji, S., Pu, J., Sun, H., Wang, L., 2020. Benzotriazole alleviates copper mediated lysosomal membrane damage and antioxidant defense system responses in earthworms (Eisenia fetida). Ecotoxicol. Environ. Saf. 197, 110618.

Zhou, Y., Liu, H., Li, J., Xu, S., Li, Y., Zhao, H., Jin, H., Liu, W., Chung, A.C.K., Hong, Y., Sun, X., Jiang, Y., Zhang, W., Fang, J., Xia, W., Cai, Z., 2018. Profiles, variability, and predictors of urinary benzotriazoles and benzothiazoles in pregnant women from WuhanChina. 121, 1279–1288.

Zhou, Y., Qu, J., Liu, W., Liao, J., Li, Y., Zhao, H., Li, J., Jin, H., Liu, H., Fang, J., Sun, X., Jiang, Y., Xu, S., Li, Y., Hong, Y., Xia, W., Cai, Z., 2020. Early pregnancy exposure to benzotriazoles and benzothiazoles in relation to gestational diabetes mellitus: a prospective cohort study. Environ. Int. 135, 105360.